References

BERGHUIS, J., HAANAPPEL, IJ. M., POTTERS, M., LOOP-STRA, B. O., MACGILLAVRY, C. H. & VEENENDAAL, A. L. (1955). *Acta Cryst.* 8, 478.

BRAGG, W. L. & WEST, J. (1929). *Z. Kristallogr.* 69, 118.

BROUSSARD, L. & SHOEMAKER, D. P. (1960). *J. Amer. Chem. Soc.* 82, 1041.

DENT, L. S. & SMITH, J. V. (1958). *Nature, Lond.* 181, 1794.

DUCROS, P. (1960). *Bull. Soc. franç. Minér. Crist.* 83, 85.

FISCHER, K. (1960). *Fortschr. Min.* 38, 201.

GARDEN, L. A., KINGTON, G. L. & LAING, W. (1955). *Trans. Faraday Soc.* 51, 1558.

HEWETT, D. F., SHANNON, E. V. & GONYER, F. A. (1928). *Proc. U. S. nat. Mus.* 73, article 16.

HOWELL, P. A. (1960). *Acta Cryst.* 13, 737.

KINGTON, G. L. & LAING, W. (1955). *Trans. Faraday Soc.* 51, 287.

KINGTON, G. L. & MACLEOD, A. C. (1959). *Trans. Faraday Soc.* 55, 1799.

MAJER, V. (1953). *Yugoslav. Akad. Znanosti i Umjetnosti*, p. 175.

NOWACKI, W., KOYAMA, H. & MLADECK, M. H. (1958). *Experientia*, 14, 396.

REED, T. B. & BRECK, D. W. (1956). *J. Amer. Chem. Soc.* 78, 5972.

SMITH, J. V. (1954). *Acta Cryst.* 7, 479.

STRUNZ, H. (1956). *Neues Jb. Miner. Mh.* 11, 250.

VENTRIGLIA, V. (1953). *Rend. Soc. Miner. Ital.* 9, 268.

WALKER, G. P. L. (1951). *Miner. Mag.* 29, 773.

WEIGEL, O. & BEZNER, E. (1927). *S.B. Ges. Naturw. Marburg*, 62, 57.

WINCHELL, A. N. & WINCHELL, H. (1951). *Elements of Optical Mineralogy*: Part II. *Description of Minerals*. Fourth edition. New York: Wiley.

WYART, J. (1933). *Bull. Soc. franç. Minér. Crist.* 56, 81.

Structure and Structure Imperfections of Solid β-Oxygen

BY ERWIN M. HÖRL

*National Bureau of Standards, Washington, D.C., U.S.A. and
Howard University, Washington, D.C., U.S.A.*

Electron diffraction studies were carried out on thin films of solid oxygen. The structure of β-oxygen was investigated and a rhombohedral structure of the space group $R\bar{3}m$ found. Its corresponding hexagonal cell has the dimensions $a = 3\cdot307 \pm 0\cdot008$, $c = 11\cdot256 \pm 0\cdot015$ Å and contains three O_2 molecules with their axis parallel to the hexagonal axis and their centers at the positions: $(\frac{1}{3}, \frac{1}{3}, 0)$, $(-\frac{1}{3}, 0, \frac{1}{3})$ and $(0, -\frac{1}{3}, \frac{2}{3})$. Faults in the stacking sequence of the $(00 \cdot l)$ layers were observed and the experimental results compared with the Paterson treatment of growth faults in f.c.c. crystals.

Introduction

Solid oxygen is known to have three modifications: an α-modification, stable up to 23·9 °K., a β-modification stable between 23·9 and 43·6 °K. and a γ-modification stable between 43·6 °K. and the melting point at 54·4 °K.

A series of attempts have been made to investigate the crystal structures and cell dimensions of these modifications using X-ray techniques. McLennan & Wilhelm (1927) were the first to carry out a structure investigation on a polycrystalline oxygen sample. At 20 °K. they found an orthorhombic cell ($a = 5\cdot50$, $b = 3\cdot82$, $c = 3\cdot44$ Å) containing two molecules. Ruhemann (1932) observed powder patterns of the α-modification (at 16 °K.), of the β-modification (at 29 °K.) and also of the γ-modification. Ruhemann's patterns of the α- and β-modification were very similar. He therefore concluded, that the α–β transition changes the structure only very little, but still noticeably. Furthermore, his patterns of α- and β-oxygen showed lines which he could not explain by the assumption of an orthorhombic cell. This led him to the conclusion, that McLennan's & Wilhelm's cell may come very close to reality, but still cannot be regarded as the real cell for the α- and β-structure. For the γ-modification he suggested the possibility of a hexagonal close packed structure. Mooy (1932) carried out investigations on α-oxygen at 20·5 °K. and found a hexagonal structure ($a = 5\cdot75$, $c = 7\cdot59$ Å) with 12 atoms per cell. Vegard (1935) reported investigations on the β- and γ-modification. He was led to the conclusion, that an orthorhombic cell cannot be the right one for the β-modification and interpreted his diffraction patterns on the basis of a rhombohedral cell ($a = 6\cdot19$ Å and $\varphi = 99\cdot1°$) with 6 molecules in undetermined positions. For the γ-modification he found a face centered arrangement of O_2–O_2 complexes, with the symmetry of the $Pa3$ space group. This result for γ-oxygen was also obtained by Keesom & Taconis (1936). Recently, Black *et al.* (1958) published X-ray diffractometer patterns of solid ozone and the three modifications of solid oxygen in connection with the description of a low temperature X-ray

diffractometer. Bolz *et al.* (1960) extended this work; their pattern of β-oxygen is discussed later.

The conflicting literature on the crystal structures of α- and β-oxygen suggested a reinvestigation using an electron diffraction technique previously developed by the author for the study of thin films of solid α-nitrogen (Hörl, 1959; Hörl & Marton, 1961). Further, it was thought to be desirable to obtain information about preferred orientation and faults of the microcrystallites in thin oxygen films.

This paper will deal primarily with experiments on thin films of β-oxygen, but some results on α-oxygen films are also given.

Experimental technique and experimental results

The technique employed in our experiments on thin films of solid oxygen consisted of transmission electron diffraction and was, as mentioned previously, essentially the same as the one used by the author in the study of thin layers of solid α-nitrogen (Hörl, 1959; Hörl & Marton, 1961).

Oxygen gas is condensed upon a thin supporting foil of aluminum or collodion mounted on a copper target block cooled by liquid hydrogen to a temperature of 20 °K. An electron beam of 46 kV. passes through the supporting foil and the layer of the solidified oxygen gas perpendicularly or at smaller angles of incidence. The electron diffraction pattern can be observed visually on a fluorescent screen or photographed.

We can divide our experiments into two groups in respect to the experimental procedure employed and the results obtained:

1. Low gas flow rate, low electron beam intensity experiments

In these experiments low gas flow rates were used during the film deposition process. These rates corresponded to layer build up speeds of 10–12 Å/sec. or approximately 3 monolayers of mol./sec. Further, the electron diffraction patterns were recorded at very low electron beam intensities to avoid heating the oxygen film above the α–β transition point at 23·9 °K. The diffraction patterns consisted of four almost equally spaced rings close together with different widths and intensities (rings 2, 3, 4 and 5 of Fig. 1) and three very weak rings of considerably larger diameters. There was strong preferred orientation of the microcrystallites present, which was revealed by patterns taken at angles of beam incidence $<90°$. The d-values, intensities and ring widths of a pattern taken at 90° beam incidence are given in Table 1. The film thicknesses were estimated to be between 300–400 Å. The patterns of these films are believed to be those of the α-modification.

2. High gas flow rate, high electron beam intensity experiments

In this case gas flow rates were employed which were an order of magnitude higher than the ones stated above. In addition, the diffraction patterns were observed and recorded with high electron beam intensities. The diffraction patterns consisted again of a series of rings with different widths and intensities. Their d-values were completely different from the ones of case 1 with the exception of two rings. No preferred orientation was detectable by rotation of the specimen

Table 1. *d-Values, relative intensities and relative half-widths of the observed diffraction rings*

	α-Oxygen (1)			β-Oxygen (2)		
Ring no.	d (Å)	Intensity (3)	Half-width (3)	d (Å)	Intensity (3)	Half-width (3)
1				3·752	1000	1
2	3·31	100	1	3·3 (4)	<10	1
3	3·11	30	1			
4	2·91	70	1·5–2			
5	2·77	50	1	2·769	≈ 5000	1·5–2
6	2·20 (4)	$\lesssim 10$	1·5(?)			
7				2·568 (4)	600	2
8				1·875$_5$	100	1
9	1·79 (4)	$\lesssim 10$	1·5(?)			
10				1·652	1000	2–3
11				1·515	150	2
12	1·46 (4)	$\lesssim 10$	1·5(?)			
13				} 1·408$_4$ (5) {	300	2·5
14					300	2·5–3·5
15				1·251 (4)	≈ 50	2
16				1·076–1·040 (6)	≈ 20	4–5
17				0·993 (4)	≈ 10	2

(1) Preferred crystal orientation; electron beam $\perp$ foil.
(2) Random crystal orientation.
(3) Eye estimates.
(4) Value has low accuracy due to faintness or diffuseness of ring.
(5) The splitting into rings no. 13 and no. 14 can barely be seen by eye. This d-value represents the measured center of the combined rings.
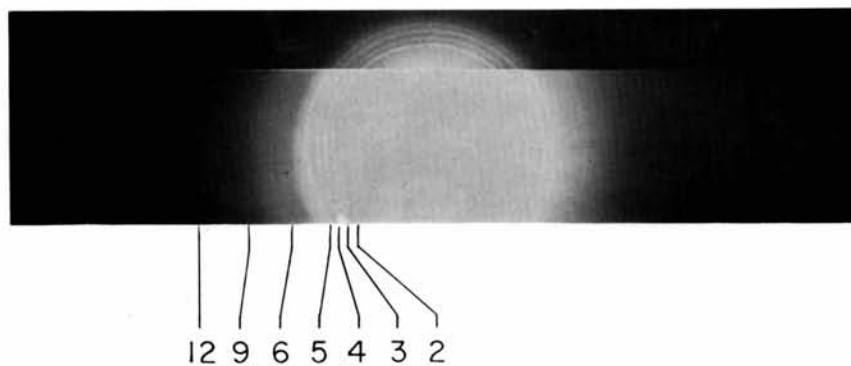(6) Range in which $I > I$(max.)/2.

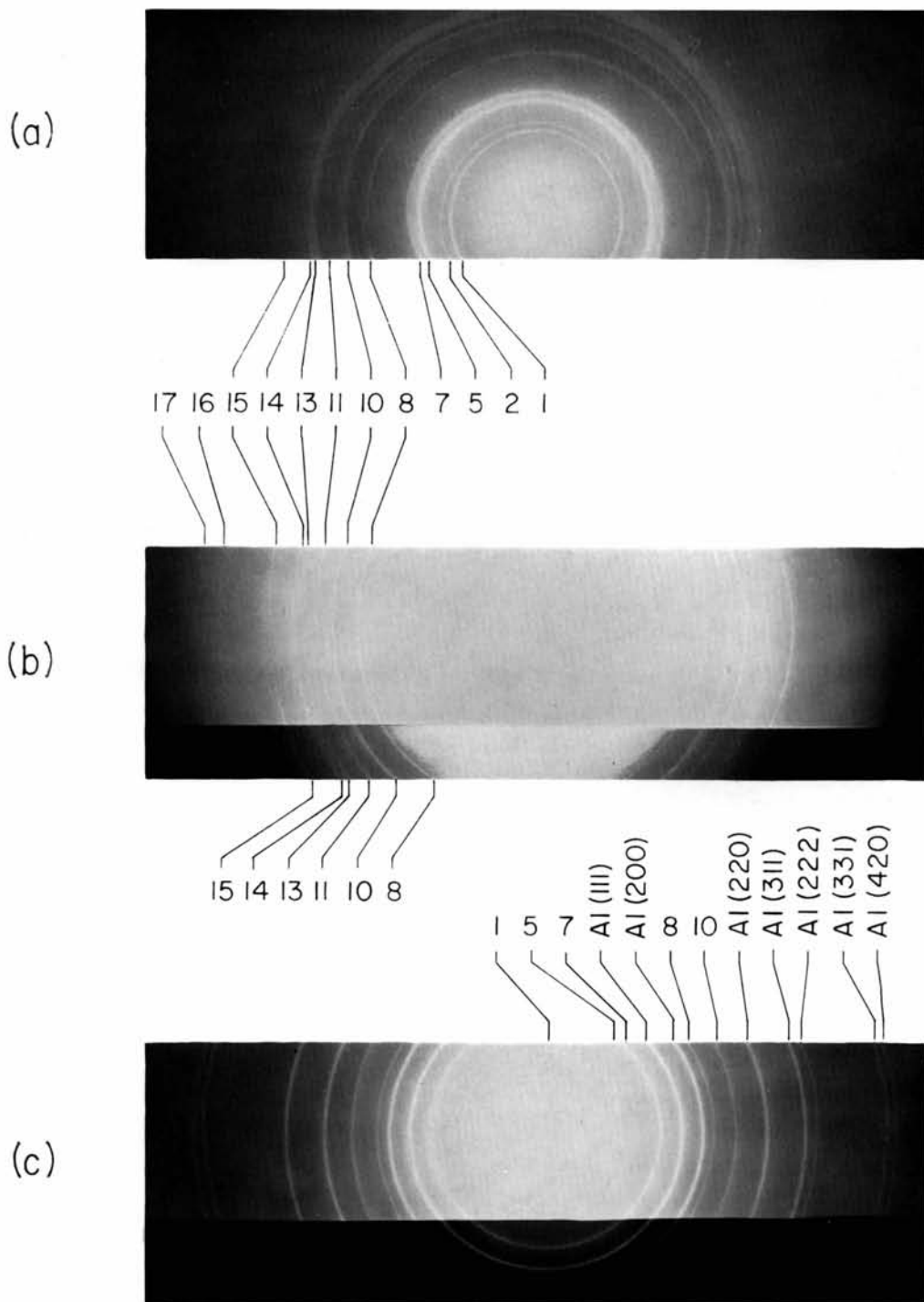Fig. 1. α-Oxygen pattern. Collodion substrate. Electron beam ⊥ foil.

Fig. 2. β-Oxygen patterns. (a) and (b) show patterns of oxygen films on collodion substrates, (c) shows a pattern on an aluminum substrate. (b) and (c) have two portions with different exposure times. For (b) the exposure times are considerably larger than the exposure time used for obtaining pattern (a).

in the electron beam. The characteristic values for a pattern of this kind are also given in Table 1. Photographs of such patterns are shown in Fig. 2. The film thicknesses were estimated to be 2–5 times larger than in case 1. The patterns of case 2 are believed to belong to the β-modification.

It is important to mention a sharpening of ring no. 7 of the β-oxygen pattern with time during a 'beam-on' period. This indicates an annealing process, which will be discussed later.

We also have to mention, that ring no. 2—the most intense ring in the α-pattern—still appears as a faint ring in the β-pattern. This is probably due to some α-oxygen crystals still present in the β-oxygen films. The reverse case may account for ring no. 5 of the α-oxygen pattern.

The temperature of the α-oxygen films must have assumed a value in the range between 20 °K. (bath temperature) and 23·9 °K. (transition temperature). The temperature of the β-oxygen films could be estimated to be not larger than approximately 28 °K., since at this temperature the deposit would have migrated or evaporated off the substrate according to our previous experience with solid nitrogen films. Most probably the actual temperature of the β-oxygen films was a few degrees above the transition point.

In all cases, the thickness of the supporting foil was small enough so that the observed diffraction patterns were simple superpositions of the patterns which would have been observed for the supporting foil or the oxygen film alone.

The d-values of the oxygen patterns were obtained by the comparison of the diameters of the oxygen diffraction rings with the diameters of the aluminum diffraction rings. The d-values for the aluminum rings on the other hand were obtained by depositing MgO on these aluminum foils and measuring the two superimposed patterns at room temperature, assuming a lattice parameter for MgO equal to 4·213 Å (Swanson & Tatge, Nat. Bur. Stand. Circular 539, Vol. 1). The data given by Figgins, Jones & Riley (1956) were used for taking into account the temperature dependence of the lattice parameter of aluminum.

The oxygen gas used according to the commercial supplier, had as main impurities $\lessgtr 0·01\%$ argon and nitrogen.

Discussion and interpretation of the β-oxygen patterns

Cell dimensions and crystal structure

Since the patterns obtained in the way described above showed random orientation of the microcrystallites, a crystal structure analysis could be carried out for β-oxygen. Hull-Davy charts for tetragonal crystals and Bunn charts for hexagonal crystals were used in the search for the cell dimensions. The best fit of the experimental data was obtained for a hexagonal cell with $a = 3·307 \pm 0·008$ and $c =$

11·256 $\pm$ 0·015 Å. The errors indicated are most probable errors, which were obtained from three sets of independent measurements, each set consisting of five to ten measurements. The indices of the diffraction rings are given in Table 2. The hexagonal cell must contain three O_2 molecules to give a calculated density of 1·495 g.cm.$^{-3}$ in agreement with the measured value of 1·426 at 20 °K. (*International Critical Tables*, Vol. 1).

In order to determine the positions of the oxygen molecules we have to look for possible extinctions and can readily establish the symmetry element 3_1 or 6_2 (or their enantiomorphs 3_2 or 6_4) through the observed condition for $00 \cdot h_3 : h_3 = 3n$. This limits the discussion to the space groups containing these symmetry elements: $P6_2$, $P6_222$, $P3_1$, $P3_112$, $P3_121$ (or their enantiomorphic groups $P6_4$, $P6_422$, $P3_2$, $P3_212$, $P3_221$), $R3$, $R\bar{3}$, $R32$, $R3m$, $R3c$, $R\bar{3}m$ and $R\bar{3}c$.

$P6_2$: In this space group we have in the case (c)† six equivalent positions suitable for three O_2 molecules. We obtain a structure factor for the $10 \cdot h_3$-group of reflecting planes of

$$\Sigma(FF^*)_{10 \cdot h_3} \approx 1·2 \cos 2\varphi + 15·5 \ddagger$$

for $h_3 \neq 3n$, and

$$\Sigma(FF^*)_{10 \cdot h_3} \approx 160$$

for $h_3 = 3n$. n is an integer $\neq 0$.
For the 11·0 group we obtain

$$\Sigma(FF^*)_{11 \cdot 0} < 1 .$$

Since 10·1, 10·2 and 11·0 are observed to be very strong reflections and 10·3 could not be detected at all, case (c) has to be excluded.

The cases (b) and (a) would also be suitable for a structure containing three O_2-molecules per unit cell. But we have to exclude them since they yield:

(b): $\Sigma(FF^*)_{00 \cdot 3} = \frac{3}{2}\Sigma(FF^*)_{10 \cdot 3} \approx 3\Sigma(FF^*)_{10 \cdot 0} = 72$

(a): $\Sigma(FF^*)_{10 \cdot 1} = \Sigma(FF^*)_{10 \cdot 2} = 0$, $\Sigma(FF^*)_{10 \cdot 3} = 122$

contrary to the observed intensities (see Table 1).

$P6_222$: The special cases (j), (i), (h), (g), (f) and (e) would have six equivalent positions suitable for the arrangement of three diatomic molecules, but do of course yield only structures already included in the discussion of $P6_2$.

$P3_1$, $P3_112$ and $P3_121$: in $P3_1$ we have three equivalent positions. We can therefore place six oxygen atoms in the positions:

$x - \xi$,	$y - \eta$,	$-\zeta$
$x + \xi$,	$y + \eta$,	$+\zeta$
$-y + \eta$,	$x - y - \xi + \eta$,	$\frac{1}{3} - \zeta$
$-y - \eta$,	$x - y + \xi - \eta$,	$\frac{1}{3} + \zeta$
$y - x - \eta + \xi$,	$-x + \xi$,	$\frac{2}{3} - \zeta$
$y - x + \eta - \xi$,	$-x - \xi$,	$\frac{2}{3} + \zeta$

---

† Small letters in brackets mean Wyckoff notation.
‡ φ: Angle between y-axis and molecule axis.

Table 2. *Experimental and theoretical data for the β-oxygen structure*

Group of reflecting planes	Ring no.	Observed* rel. intensity	Observed* rel. half-width	Structure factor (incl. multipl. factor) molecular axis || z-axis	Structure factor (incl. multipl. factor) free rotating molecules	Calculated rel. intensity†	Calculated d-value	Effect of stacking faults
00·1		0		0·0	0·0	0		
00·2		0		0·0	0·0	0		
00·3	1	1000	1	20·3	72·0	820	3·752	none
10·0		0		0·0	0·0	0		
00·4		0		0·0	0·0	0		
10·1	5	≈ 5000	1·5–2	192·4	216·0	4700	2·775	eff.
10·2	7	600	2	131·9	216·0	2300	2·554	eff.
10·3		0		0·0	0·0	0		
00·5		0		0·0	0·0	0		
10·4		0		10·5	216·0	80	2·008	eff.
00·6	8	100	1	13·7	72·0	78	1·877	none
10·5		0		2·8	216·0	12	1·771	eff.
11·0	10	1000	2–3	216·0	216·0	740	1·654	none
11·1		0		0·0	0·0	0		
00·7		0		0·0	0·0	0		
11·2		0		0·0	0·0	0		
10·6		0		0·0	0·0	0		
11·3	11	150	2	121·8	432·0	280	1·513	none
20·0		0		0·0	0·0	0		
11·4 } 20·1 }	13	300	2·5	0·0 / 192·4	0·0 / 216·0	0 / 340	1·421	eff.
00·8		0		0·0	0·0	0		
10·7 } 20·2 }	14	300	2·5–3·5	108·6 / 131·9	216·0 / 216·0	180 / 210	1·403 / 1·389	eff. / eff.
20·3		0		0·0	0·0	0		
11·5		0		0·0	0·0	0		
20·4		0		10·5	216·0	11	1·277	eff.
10·8 } 00·9 } 11·6 }	15	≈ 50‡	2	175·9 / 71·2 / 82·1	216·0 / 72·0 / 432·0	180 / 71 / 78	1·263 / 1·251 / 1·241	eff. / none / none
20·5		0		2·8	216·0	2	1·208	eff.
11·7		0		0·0	0·0	0		
10·9		0		0·0	0·0	0		
20·6		0		0·0	0·0	0		
00·10		0		0·0	0·0	0		
21·0		0		0·0	0·0	0		
21·1 } 20·7 } 11·8 } 21·2 } 10·10 }	16	≈ 20‡	4–5	384·8 / 108·6 / 0·0 / 263·7 / 204·9	432·0 / 216·0 / 0·0 / 432·0 / 216·0	180 / 51 / 0 / 120 / 87	1·078 / 1·070 / 1·063 / 1·048	eff. / eff. / eff. / eff.
21·3		0		0·0	0·0	0		
00·11		0		0·0	0·0	0		
21·4		0		21·1	432·0	8	1·010	eff.
20·8		0		175·9	216·0	60	1·004	eff.
11·9	17	≈ 10‡	2	426·9	432·0	140	0·998	none

* Eye estimates.

† Based on the structure factors given in column 5 and the atomic scattering factors for oxygen given by Peiser *et al.* (1955).

‡ The observed decrease of intensity at large angles was much stronger than predicted by the simple kinematic theory used in the calculation of the intensities of column 7. An explanation for this phenomenon may be found in the non-validity of the kinematic approach due to the considerably large foil thickness.

where $x, y, 0$ are the coordinates of the center of the first molecule, ξ, η, ζ are the coordinates of one of the atoms of the first molecule relative to the molecule center. For ζ the following relationship exists:

$$\zeta = [D^2/4 - (\xi^2 + \eta^2 - \xi\eta)a^2]^{\frac{1}{2}}/c$$

where D is the internuclear distance of the O_2 molecule in the crystal.†

_____

† We have used in all our structure factor calculations as D the gas phase value of the O_2 molecule in the ground state:

Thus structure factors depend on the four parameters x, y, ξ and η, which have to be varied independently to obtain the factors for all possible molecular arrangements. A program for the IBM 704 computer was designed and about 2000 values of

_____

$1\cdot20741 \pm 0\cdot00002$ Å (Sutton *et al.*, 1958), since D for the solid state is expected to be only very little different from the gas phase value. A variation of $D/2c$ by $\pm 1\%$ yielded for the final structure intensities, which are still well comparable with the eye estimates of the intensities of the observed diffraction rings.

structure factors calculated, containing the values for the molecular arrangements with the higher symmetry of $P3_112$ and $P3_121$ and the values for the arrangements $x=\frac{1}{3}$, $y=\frac{1}{3}$, ξ, $\eta=0$. A quite good agreement between the observed and calculated diffraction ring intensities could be obtained for the molecular arrangement $x=y=\frac{1}{3}$ and $\xi=\eta=0$ of $R\overline{3}m$, which is a special case of the arrangements of $P3_121$. No other agreement between the observed and calculated intensities could be detected. No further search in the space group $P3_1$ was carried out, since the low symmetry of this group does not seem very suitable for a crystal containing only simple diatomic molecules with atoms of the same kind.

$R3$, $R\overline{3}$, $R32$, $R3m$, $R3c$, $R\overline{3}m$ and $R\overline{3}c$: These space groups are either not suitable for three O_2 molecules per hexagonal unit cell or are already included as special cases in the discussion of the trigonal groups $P3_1$, $P3_112$ and $P3_121$.

Our space group analysis thus has yielded only one possible structure with the centers of the molecules at the positions $(\frac{1}{3}, \frac{1}{3}, 0)$, $(-\frac{1}{3}, 0, \frac{1}{3})$ and $(0, -\frac{1}{3}, \frac{2}{3})$ and the axis of the molecules parallel to the z-axis. This structure, of course, could equally well be described by a rhombohedral cell ($a_R = 4\cdot210 \pm 0\cdot07$ Å, $\varphi = 46° \; 16' \pm 9'$) containing one molecule parallel to the trigonal axis. The calculated density is $1\cdot495$ g.cm.$^{-3}$, the minimum distance between two oxygen atoms belonging to different molecules is $3\cdot182$ Å. The structure factors of this structure are given in column 5 of Table 2. Column 6 of Table 2 shows the structure factors for the case of free rotating molecules (molecules treated as single scattering centers). The agreement between the observed intensities (Table 2, column 3) and the calculated intensities (Table 2, column 7) is quite good. Major disagreement exists only for the groups of reflecting planes 10·2 and 10·4.

The low value for the intensity of 10·2 is most probably due to the existence of stacking faults, since the intensity of 10·2 changes during annealing of the sample. This will be discussed further at the end of the following chapter. A parallel case was observed for the 200 reflection of solid α-nitrogen (Hörl & Marton, 1961).

The absence of the 10·4 diffraction ring is a more serious problem. The theory of stacking faults (see below) predicts a diffuse 10·4 ring with an intensity maximum smaller than the intensity maximum for the perfect structure. Since the effect of stacking faults on diffraction rings can be very strong (see discussion of 10·2 in following section), it could very well be that stacking faults are the reason for an unobservable low intensity of this diffraction ring.

There was no experimental evidence for a preferred alignment of the microcrystallites in the β-oxygen films. In spite of this fact, we investigated the change of intensity to be expected for the 10·4 and the neighboring 00·6 diffraction ring for the most probable type of a partial preferred alignment: (00·1)||subtrate.

Such an alignment would in fact reduce the intensity of 10·4 considerably, but the intensity of 00·6 should be reduced even more. Since the 00·6 was very clearly visible this type of preferred alignment cannot be assumed to account for the non-appearance of 10·4.

Another possible explanation for the non-appearance of 10·4 may lie in hindered rotations of the molecules. This suggests the investigation of the far infrared adsorption spectrum of solid β-oxygen.

We also have searched through the X-ray work on solid β-oxygen for an X-ray diffraction line with the d-value of our expected 10·4 ring. And indeed Vegard reports two very weak lines of equal intensity at positions corresponding to our 10·4 and 00·6 rings. On the other hand, Ruhemann observes only a weak line corresponding to our 00·6 ring, but no line at the position where the 10·4 ring should be visible. Bolz et al. (1960) have detected a weak line at $d = 2\cdot01$ Å, which corresponds to our calculated 10·4 d-value.

Stacking faults

The observed diffraction patterns consist of diffuse and sharp rings, which suggest very much an interpretation in terms of growth faults in the stacking of (00·l)-layers. We can readily apply the theory of growth faults in f.c.c. crystals, as developed by Paterson (1952) if we simplify the problem and treat the O_2-molecules as free rotating about their centers i.e. as single scattering centers. According to Paterson only reflections $h_1h_2\cdot h_3$ with $h_1 - h_2 = 3N$ and $h_3 = 3N'$ are unaffected. For all other cases an elongation and shift of the high intensity regions in the reciprocal lattice takes place (see Fig. 3(a)). Column 9 of Table 2 indicates whether an effect on the line width is to be expected. Comparison of this column with column 4 yields good overall agreement between prediction and observation, except for the 11·0 and 11·3 groups, which appear diffuse and are expected to be sharp.

There is also a second discrepancy between theory and experiment. According to Paterson's results the reflections 10·1 and 10·2 should behave very similarly as the number of faults increases. Both reflections should broaden to the same extent, their maxima should move towards $h_3 = \frac{3}{2}$, and the distances of the two maxima from $h_3 = \frac{3}{2}$ should always be identical (Fig. 3(a)).

This behavior could not be observed at all. A freshly deposited oxygen film yielded a pattern with a 10·1 reflection of about two times the width of the always sharp 00·3 reflection. The 10·2 reflection was a very faint and broad halo, often barely visible (see Figs. 2(c) and 3(b)). With an electron beam of high intensity a sharpening of 10·2 occurred until its width was comparable to that of the 10·1. The intensity of 10·2 was still approximately a factor of four lower than predicted by the structure. The width of 10·1 remained unchanged.

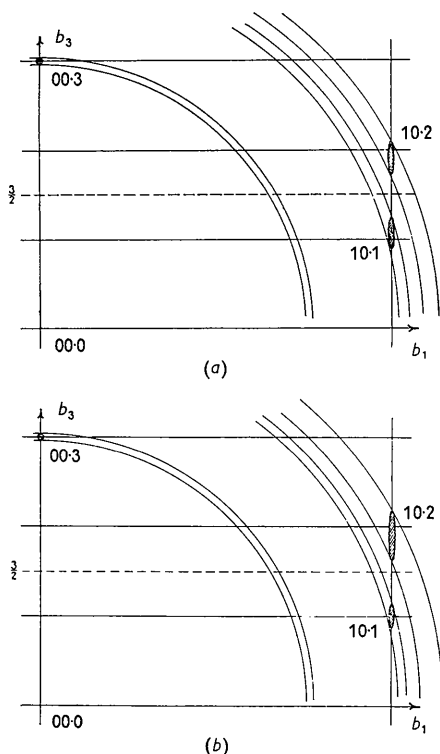These observations indicate an annealing process

Fig. 3. (01·0) plane of reciprocal lattice for β-oxygen with the first three diffraction rings indicated. (a) According to theory. Rotating molecules and growth faults in the stacking of the (00·1) crystal planes. Fault probability between 0 and $2\sqrt{3}-3$. (b) As actually observed. 10·2 ring in the process of sharpening.

due to heating of the specimen. The number of faults are gradually reduced, but the process itself does not follow the theoretical predictions outlined above.

No explanation for these discrepancies could be found. The simplification introduced by assuming molecular rotation as well as the basic assumptions in Paterson's theory may contribute to this disagreement to some extent. On the other hand, the types of faults assumed may be inappropriate.

Earlier work

In the following we will compare our observations and results with those of the early investigators.

McLennan & Wilhelm's *d*-values observed for an oxygen sample at 20 °K. agree partly with the *d*-values of our α-, partly with those of our β-patterns. This could be explained by assuming that their specimen contained a mixture of both modifications.

Mooy's pattern taken at 20 °K. and regarded as α-oxygen is very similar to our β-pattern, except for one line, which seems to correspond to one of our α-lines.

Ruhemann's patterns for α- and β-oxygen taken

at 16 and 29 °K. are—in contrast to our observations —almost identical. They resemble quite closely our β-pattern except for a few very weak lines, which we could not observe. The same situation is true for Vegard's β-pattern. Black's *et al.* β-pattern shows our first three lines. The pattern of Bolz *et al.* of the β-modification is in general agreement with our electron diffraction pattern, although there was obviously considerable preferential orientation in this case.

Since Vegard's interpretation is the latest one, we will discuss it and compare it with our results. Vegard has also found a rhombohedral structure, but his rhombohedral indices do not correspond to ours which can be derived by a well-known transformation from the hexagonal indices given in Table 2. We have checked this matter and assigned to our lines Vegard's indices. The match on the Bunn chart was not very satisfactory. A further check of Vegard's paper revealed an error in his equation for $H^2 = Q$. The factor $\sin^2\varphi/(1-3\cos^2\varphi+2\cos^3\varphi)$ should be added to the expression $(1/a^2)[h^2+k^2+l^2+C(kl+lh+hk)]$ of equation (6). Since the missing factor is close to one for angles slightly larger than 90°, Vegard's cell parameters are not very strongly affected by this error.

References

BLACK, I. A., BOLZ, L. H., BROOKS, F. P., MAUER, F. A. & PEISER, H. S. (1958). *J. Res. Nat. Bur. Stand. Wash.* **61**, 367.

BOLZ, L. H., MAUER, F. A. & PEISER, H. S. (1960). Private Communication.

FIGGINS, B. F., JONES, G. O. & RILEY, D. P. (1956). *Phil. Mag.* **8/1**, 747.

HÖRL, E. M. (1959). *Bull. Amer. Phys. Soc.* II, **4**, 221.

HÖRL, E. M. & MARTON, L. (1961). *Acta Cryst.* **14**, 11.

International Critical Tables (1926), Vol. 1, p. 104. New York.

KEESOM, W. H. & TACONIS, K. W. (1936). *Leiden Comm.* **240d**.

McLENNAN, J. C. & WILHELM, J. O. (1927). *Phil. Mag.* **7/3**, 383.

MOOY, H. H. (1932). *Leiden Comm.* **223a**.

PATERSON, M. S. (1952). *J. Appl. Phys.* **23**, 805.

PEISER, H. S., ROOKSBY, H. P. & WILSON, A. J. C. (1955). *X-ray Diffraction by Polycrystalline Materials.* London: Institute of Physics.

RUHEMANN, M. (1932). *Z. Phys.* **76**, 368.

SUTTON, L. E., *et al.* (1958). *Tables of Interatomic Distances and Configurations in Molecules.* London: The Chemical Society.

VEGARD, L. (1935). *Z. Phys.* **98**, 1.